Supplementary Information for

Microbial responses to changing plant community protect peatland carbon stores during Holocene drying

Yiming Zhang[1,2,3], Xianyu Huang[1,2*], Bingyan Zhao[1,4], Chaoyang Yan[2], Hongyan Zhao[5], Hongbin Zhang[1], Toby A. Halamka[3], Rebecca H. Peel[3], Mike Vreeken[3], Angela V. Gallego-Sala[6], Richard D. Pancost[3], Shucheng Xie[1]

[1] State Key Laboratory of Geomicrobiology and Environmental Changes, China University of Geosciences, Wuhan 430078, China

[2] Hubei Key Laboratory of Critical Zone Evolution, School of Geography and Information Engineering, China University of Geosciences, Wuhan 430078, China

[3] Organic Geochemistry Unit, School of Chemistry, and School of Earth Sciences, University of Bristol, Bristol BS8 1TS, UK

[4] Guangdong University of Petrochemical Technology, Maoming 525000, China

[5] Key Laboratory of Geographical Processes and Ecological Security in Changbai Mountains, Ministry of Education, School of Geographical Sciences, Northeast Normal University, Changchun 130024, China

[6] Department of Geography, University of Exeter, Exeter, UK

*Corresponding to: Xianyu Huang (xyhuang@cug.edu.cn)

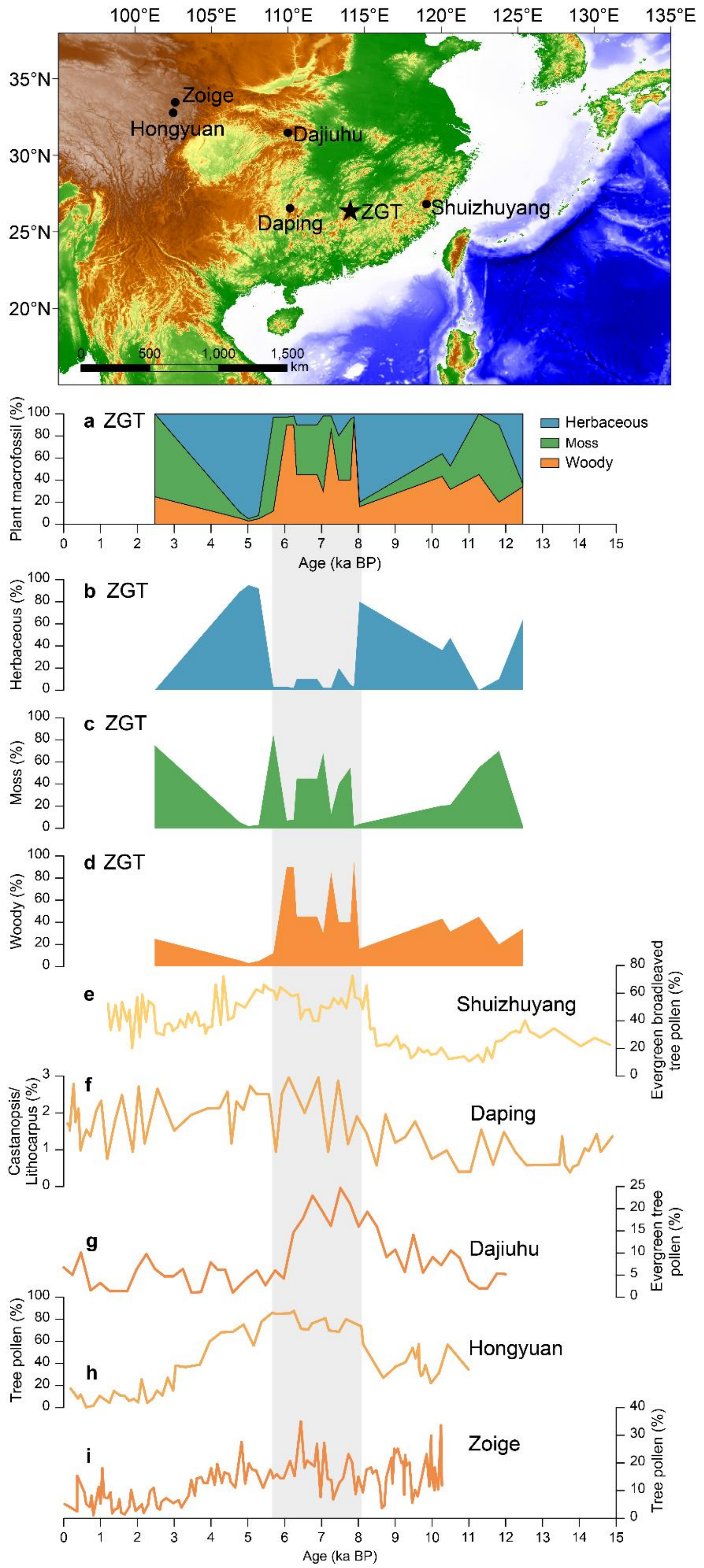

Fig. S1 Paleo-vegetation changes in ZGT peat core and pollen records in peatlands across central and southern China. The site names of curves correspond to sites shown on the map. **a**, Proportion of herbaceous, moss, and woody plant macrofossils in ZGT peat core. **b**, Proportion of herbaceous plants in ZGT peat core. **c**, Proportion of mosses in ZGT peat core. **d**, Proportion of woody plants in ZGT peat core. **e**, Proportion of evergreen broadleaf tree pollen in Shuizhuyang peatland[1]. **f**, Proportion of *Castanopsis* and *Lithocarpus* pollen in Daping peatland[2]. **g**, Proportion of evergreen tree pollen in Dajiuhu peatland[3]. **h**, Proportion of tree pollen in Hongyuan peatland[4]. **i**, Proportion of tree pollen in Zoige peatland[5]. The public elevation data are obtained from the USGS EROS Archive - Shuttle Radar Topography Mission (SRTM), provided by USGS/NASA (https://earthexplorer.usgs.gov).

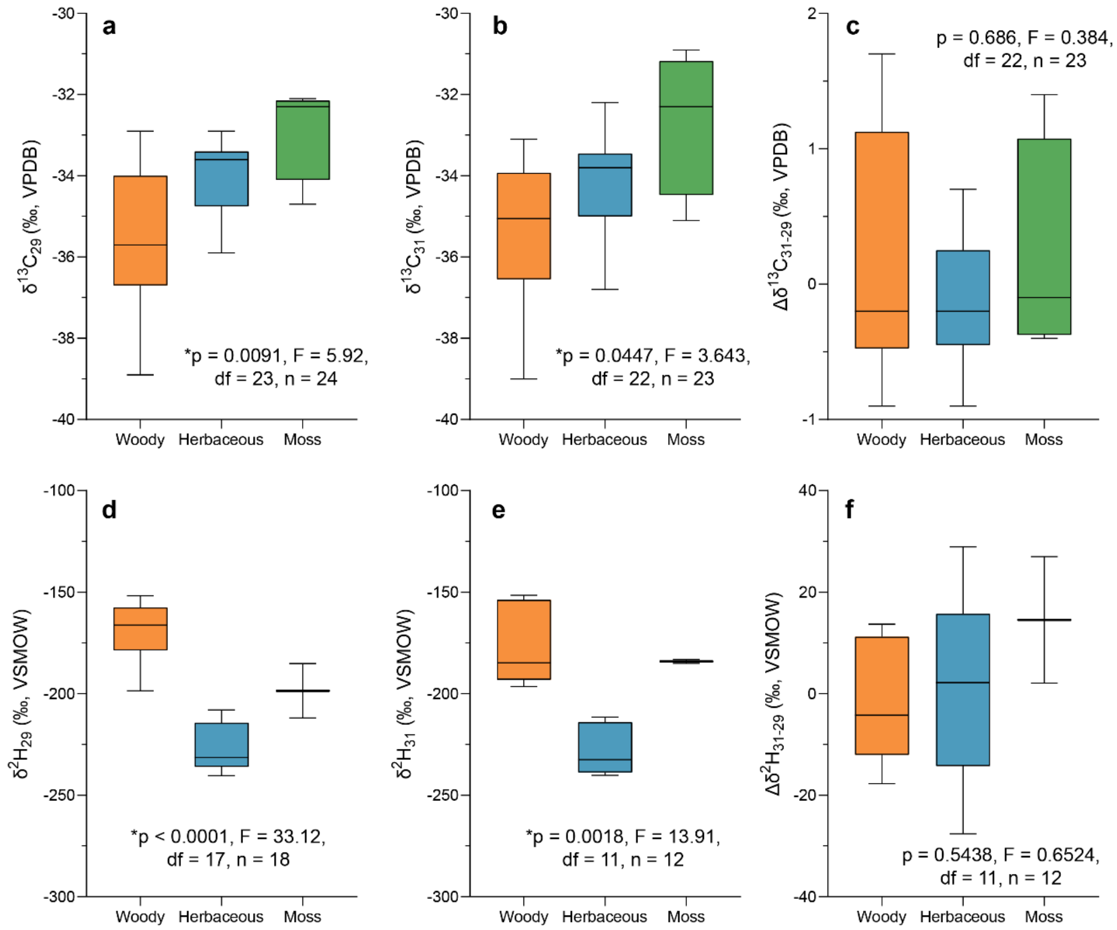

Fig. S2 Comparison of δ^{13}C and δ^{2}H values of leaf wax C_{29} and C_{31} *n*-alkanes in modern woody, herbaceous, and moss plants from ZGT peatland. **a**, The δ^{13}C values of C_{29} *n*-alkane differ significantly among the three plant types. **b**, The δ^{13}C values of C_{31} *n*-alkane differ significantly among the three plant types. **c**, The $\Delta\delta^{13}C_{31-29}$ offset do not show significant differences among the three plant types. **d**, The δ^{2}H values of C_{29} *n*-alkane differ significantly among the three plant types. **e**, The δ^{2}H values of C_{31} *n*-alkane differ significantly among the three plant types. **f**, The $\Delta\delta^{2}H_{31-29}$ offset do not show significant differences among the three plant types. One-way ANOVA was performed to assess significant differences, with p-value, F-value, degrees of freedom (df), and sample size (n) displayed in the figure. The asterisk indicates significant differences ($p < 0.05$). Box plot elements: Center line, median; box limits, upper and lower quartiles; whiskers, minimum to maximum. Species and raw data are shown in the Table S1.

Table S1 $\delta^{13}C$ and $\delta^{2}H$ values of leaf wax C_{29} and C_{31} *n*-alkanes in modern woody, herbaceous, and moss plants from ZGT peatland.

Sample ID	Species	Type	$\delta^{13}C_{29}$	$\delta^{13}C_{31}$	$\delta^{2}H_{29}$	$\delta^{2}H_{31}$
ZGT1908-P5	*Frangula crenata*	woody	-38.9	-39.0	-165.2	-151.5
ZGT1908-P7	*Frangula crenata*	woody	-34.8	-33.1	-178.4	-184.8
ZGT1908-P1	*Frangula crenata*	woody	-35.2	-35.6	-160.8	n.d.[a]
ZGT1908-P15	*Frangula crenata*	woody	-36.0	-36.1	-167.3	n.d.
ZGT1908-P17	*Rhododendron* spp.	woody	-32.9	-33.1	-178.7	-196.4
ZGT1908-P19	*Rhododendron* spp.	woody	-33.5	-34.2	-198.6	-189.8
ZGT1908-P20	*Rhododendron* spp.	woody	-34.0	-34.2	n.d.	n.d.
ZGT1908-P6	*Camellia caudata*	woody	-37.0	-37.9	-151.8	-156.0
ZGT1908-P8	*Camellia caudata*	woody	-35.8	-34.6	-156.5	n.d.
ZGT1908-P13	*Camellia caudata*	woody	-36.7	-35.5	n.d.	n.d.
ZGT1908-P21	*Camellia caudata*	woody	-35.7	n.d.	n.d.	n.d.
ZGT1908-P11	*Rhynchospora chinensis*	herbaceous	-35.9	-36.8	-234.8	-232.5
ZGT1908-P14	*Rhynchospora chinensis*	herbaceous	-35.7	-36.0	-236.5	-237.4
ZGT1908-P16	*Rhynchospora chinensis*	herbaceous	-33.4	-33.6	-208.0	n.d.
ZGT1908-P18	*Rhynchospora chinensis*	herbaceous	-33.8	-33.8	-232.5	n.d.
ZGT1908-P4	*Carex* spp.	herbaceous	-33.4	-33.9	-212.7	-240.2
ZGT1908-P3	*Carex* spp.	herbaceous	-33.6	-34.0	-230.3	n.d.
ZGT1908-P12	*Carex* spp.	herbaceous	-33.8	-33.3	-240.4	-211.5
ZGT1908-P22	*Carex* spp.	herbaceous	-33.6	-33.7	-219.0	-216.5
ZGT1908-P23	*Carex* spp.	herbaceous	-32.9	-32.2	n.d.	n.d.
ZGT1908-P2	*Sphagnum palustre*	moss	-32.3	-30.9	-212.0	-185.0
ZGT1908-P10	*Sphagnum palustre*	moss	-34.7	-35.1	-185.1	-183.1
ZGT1908-P24	*Sphagnum palustre*	moss	-32.1	-32.0	n.d.	n.d.
ZGT1908-P9	*Sphagnum palustre*	moss	-32.3	-32.6	n.d.	n.d.

[a] not detected

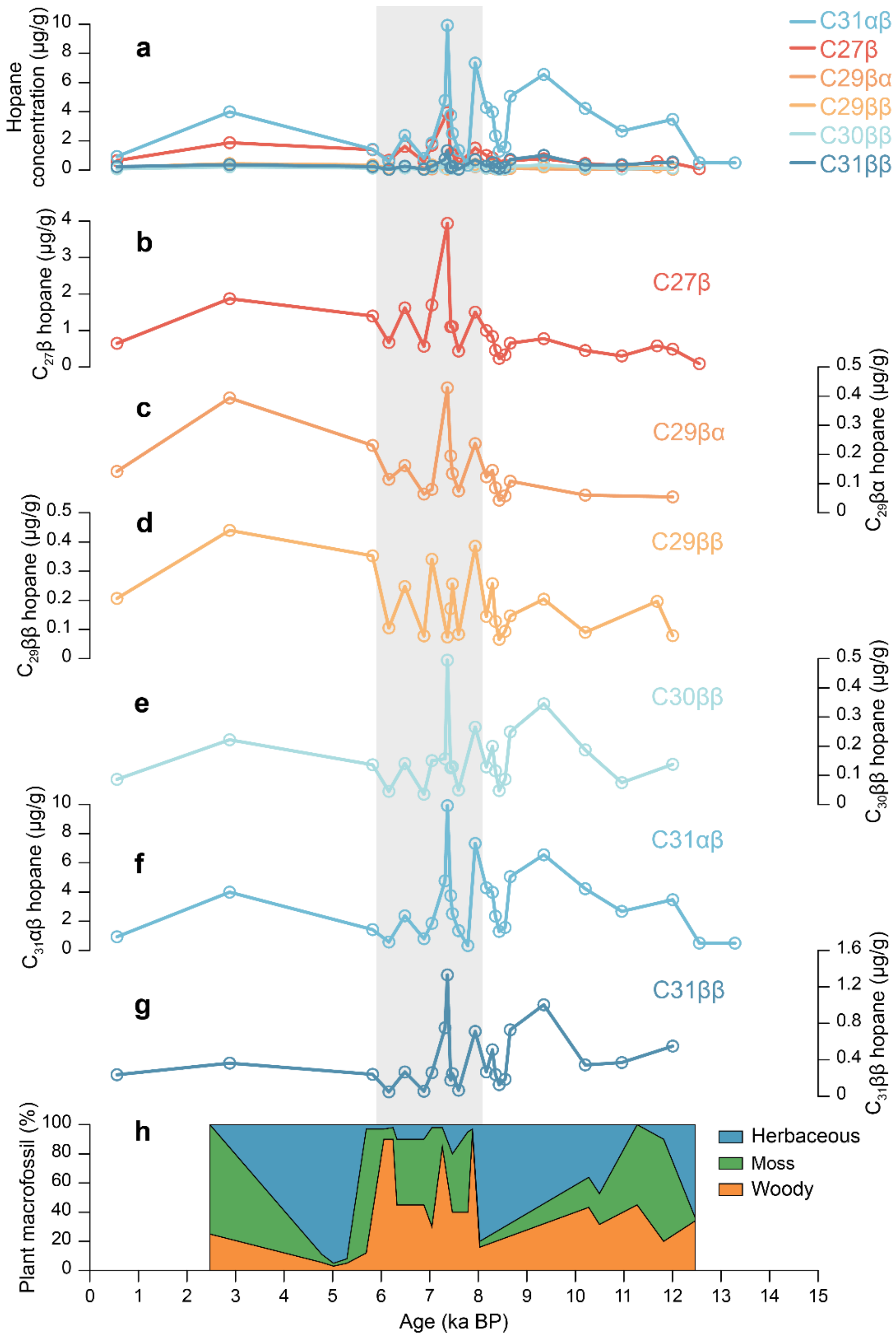

Fig. S3 Changes in bacterial hopane concentrations in ZGT core during woody plant expansion. a, Total concentration of C_{27}β, C_{29}βα, C_{29}ββ, C_{30}ββ, C_{31}αβ, and C_{31}ββ hopanes. **b-g**, Concentrations of different hopanes, with hopane types labeled on the right. **h**, Percentages of moss, herbaceous, and woody plant macrofossils in ZGT peat core.

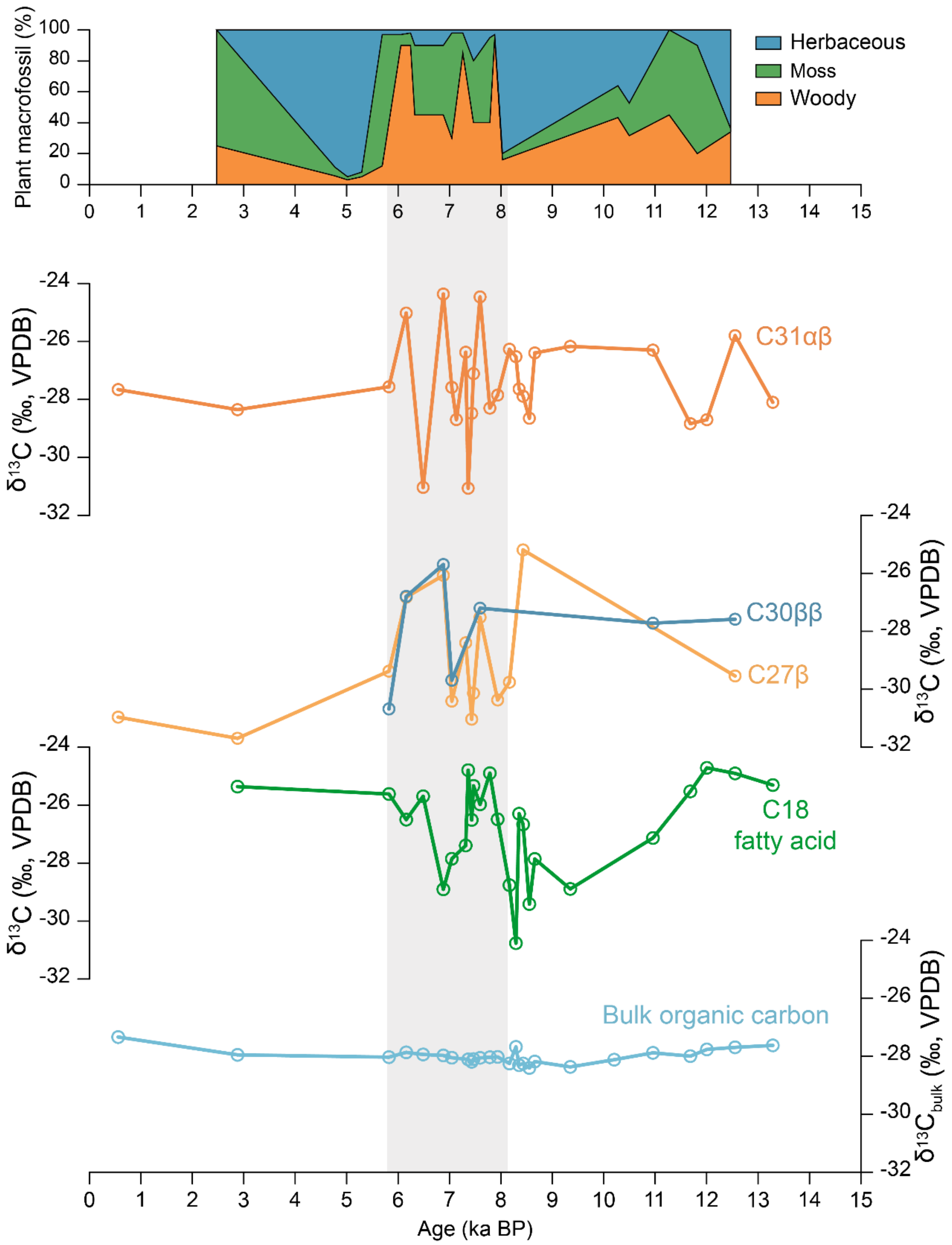

Fig. S4 Variations in δ^{13}C values of bacterial hopanoids, C_{18} fatty acid, and bulk peat organic carbon in the ZGT core during woody plant expansion.

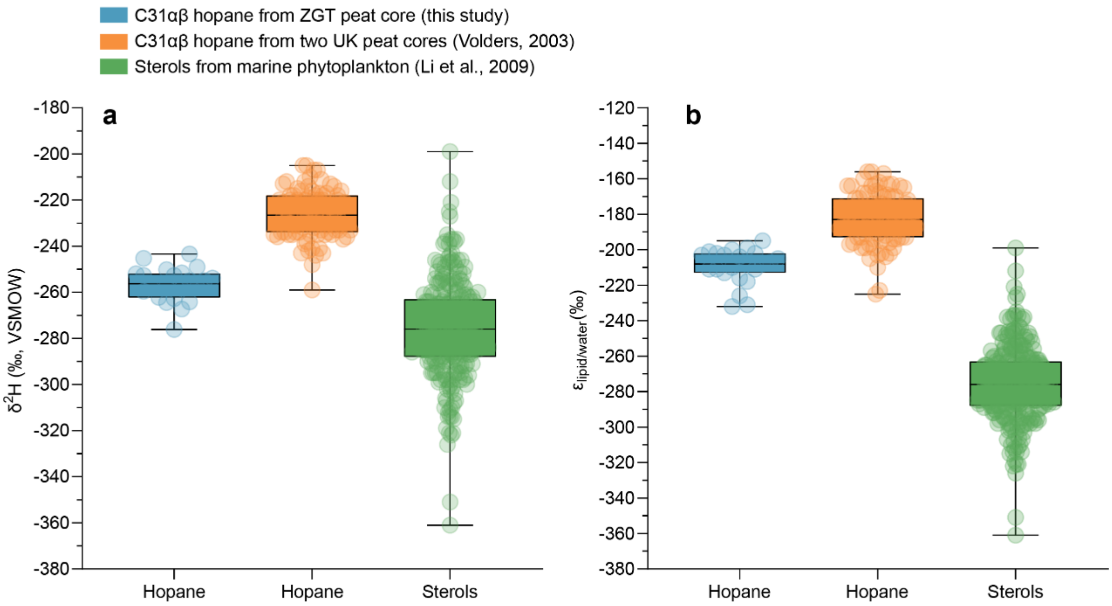

Fig. S5 Comparison of hydrogen isotope composition and fractionation of $C_{31}\alpha\beta$ hopane from peat cores with sterols from marine phytoplankton. a, The hydrogen isotope composition (δ^2H) of $C_{31}\alpha\beta$ hopane and sterols. **b**, The hydrogen isotope fractionation ($\varepsilon_{hopane/water}$) of $C_{31}\alpha\beta$ hopane and sterols. The top legend indicates the data sources. The two UK peat cores are derived from two ombrotrophic bogs, Bolton Fell Moss and Walton Moss[6]. The $\varepsilon_{lipid/water}$ values of hopane in these cores were calculated based on the source water δ^2H values inferred from the δ^2H values of *n*-alkanes within the same cores[6]. The $\varepsilon_{lipid/water}$ values of marine phytoplankton sterols were calculated assuming a seawater δ^2H value of 0‰[7]. Box plot elements: Center line, median; box limits, upper and lower quartiles; whiskers, minimum to maximum.

Our hopane δ^2H values are generally lower compared to those from peat cores in UK ombrotrophic bogs[6], and are closer to the δ^2H values observed in MVA-pathway-derived sterols produced by marine photoautotrophic phytoplankton (Supplementary Fig. S5a). Similarly, $\varepsilon_{hopane/water}$ values from the ZGT peat core are intermediate between those of hopanes from UK peat cores and marine phytoplankton sterols (Supplementary Fig. S5b). The relative lack of previous work prevents rigorous interpretation, but speculatively, the ZGT hopane $\varepsilon_{hopane/water}$ data may reflect a combination of dominant heterotrophy and partial autotrophy, with lower δ^2H ($\varepsilon_{hopane/water}$) values during woody plant expansion potentially indicating a higher contribution from autotrophy.

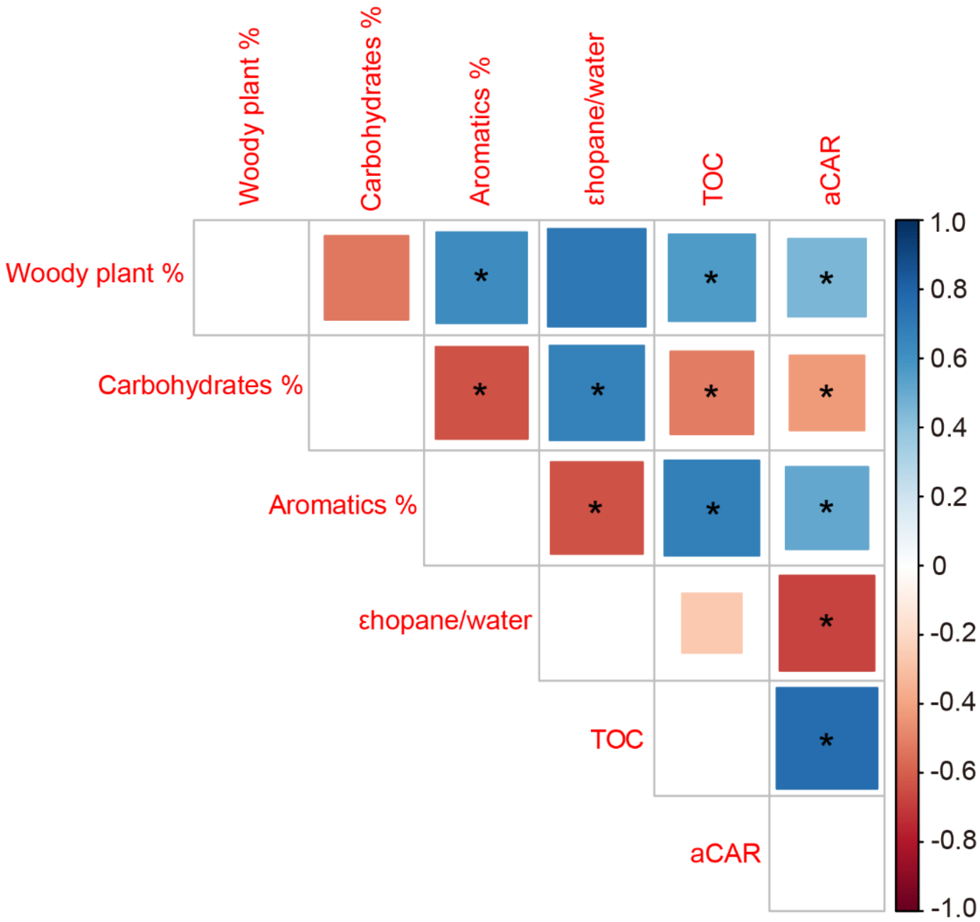

Fig. S6 Correlation heat map showing the correlation efficiencies between vegetation, peat chemistry, bacterial metabolism, and carbon dynamics in the ZGT peat core. TOC, total organic carbon content. aCAR, apparent carbon accumulation rate. The black asterisk represents significant correlations at the 0.05 levels.

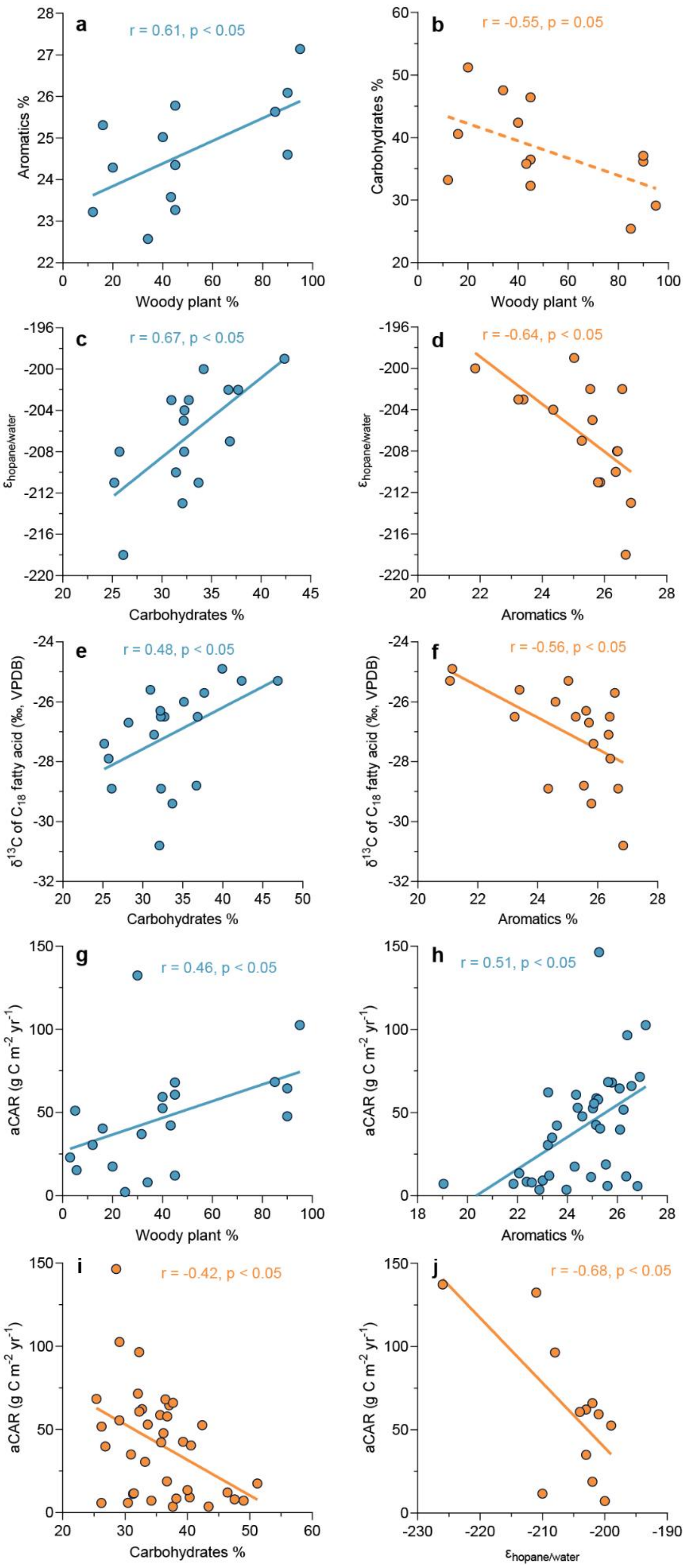

Fig. S7 Relationships between vegetation, peat chemistry, microbial metabolism, and carbon accumulation in the ZGT peat core. a, Positive correlation between woody plant macrofossil and aromatics. **b**, Negative correlation between woody plant macrofossil and carbohydrates. **c**, Positive correlation between carbohydrates and bacterial hopane $\varepsilon_{lipid/water}$. **d**, Negative correlation between aromatics and bacterial hopane $\varepsilon_{lipid/water}$. **e**, Positive correlation between carbohydrates and the $\delta^{13}C$ of C_{18} fatty acid. **f**, Negative correlation between aromatics and the $\delta^{13}C$ of C_{18} fatty acid. **g**, Positive correlation between woody plant macrofossil and apparent carbon accumulation rate. **h**, Positive correlation between aromatics and apparent carbon accumulation rate. **i**, Negative correlation between carbohydrates and apparent carbon accumulation rate. **j**, Negative correlation between bacterial hopane $\varepsilon_{lipid/water}$ and apparent carbon accumulation rate. The Pearson correlation coefficient (r) and significance p-value are displayed in the figure.

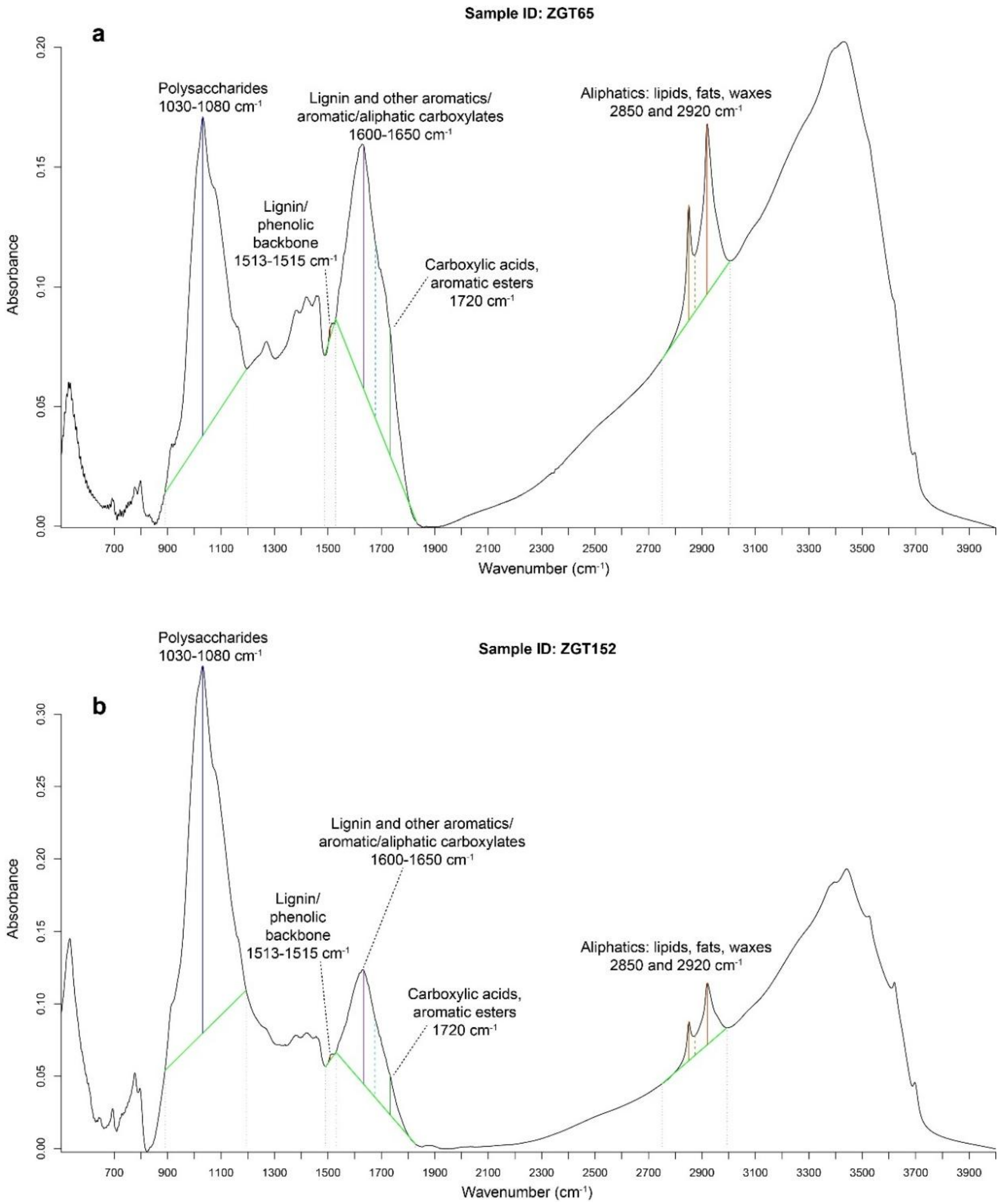

Fig. S8 Comparison of FTIR spectrum between woody plant expansion period (a) and non-woody plant expansion period (b) in the ZGT peat core.

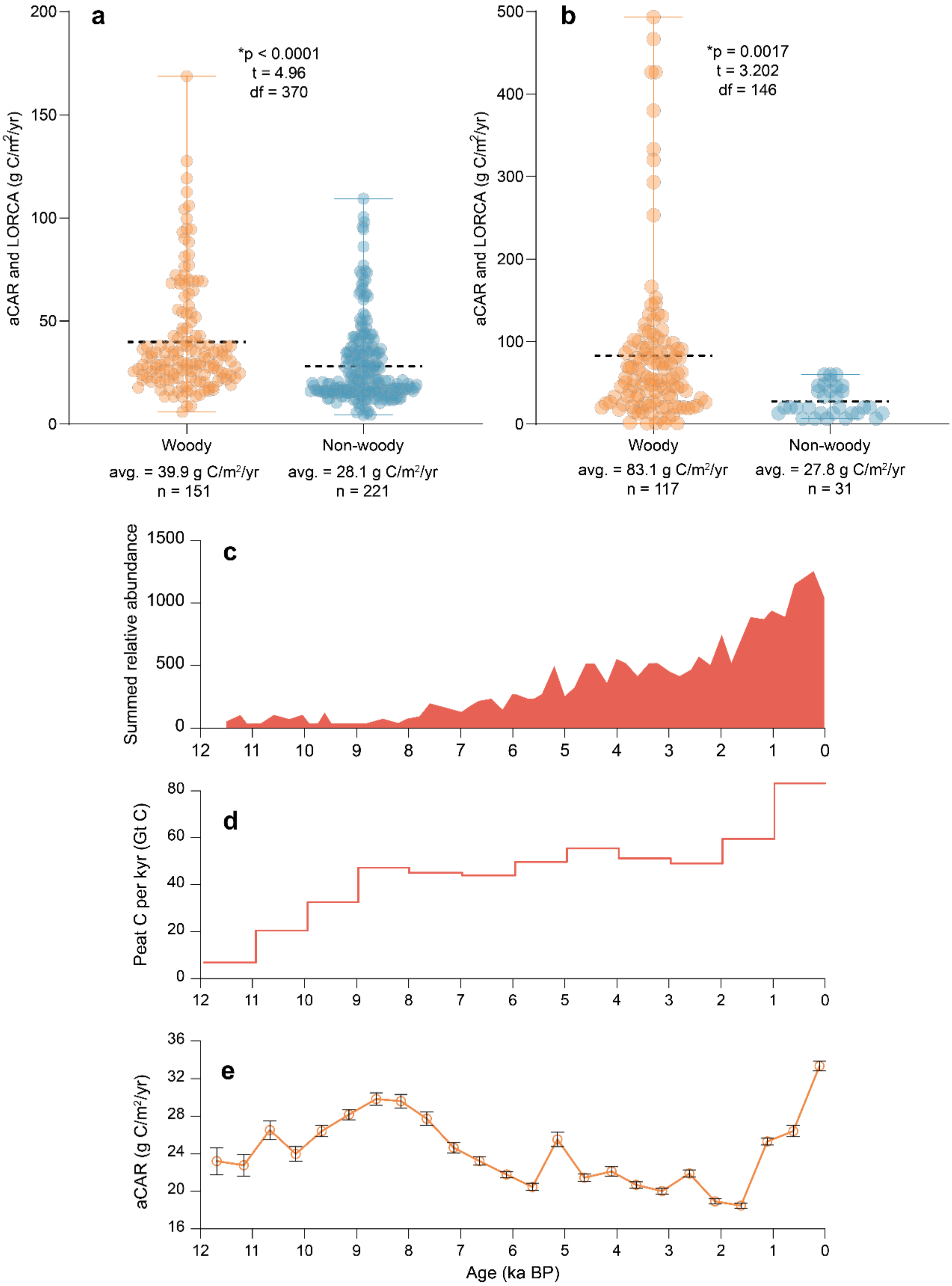

Fig. S9 Effects of woody plant on peatland carbon accumulation and net carbon pools. a, Comparison of apparent carbon accumulation rates (aCAR) and long-term apparent carbon accumulation rates (LORCA) between woody-dominated and non-woody periods in 166 peat cores from 128 northern peatlands. **b**, Comparison of aCAR and LORCA between woody-dominated and non-woody periods in 30 peat cores from 27 tropical peatlands. Horizontal dashed lines represent the average values. Note that the y-axis scale in panel b is different from that in panel a. An unpaired t-test was performed to assess significant differences, with p-value, t-value, degrees of freedom (df), and sample size (n) displayed in the figure. Peatland information and data sources are listed in the supplementary data. **c**, Summed relative abundance of woody plants in circum-Arctic peatlands presented in 200-year bins, redrawn from ref. 8. **d,** Observed net carbon pool changes for northern peatlands in 1000-year intervals, redrawn from ref. 9. **e,** Mean peat carbon accumulation rates with standard error in 500-year bins, based on 151 peat cores from 127 sites across northern peatlands, redrawn from ref. 10 and 11.

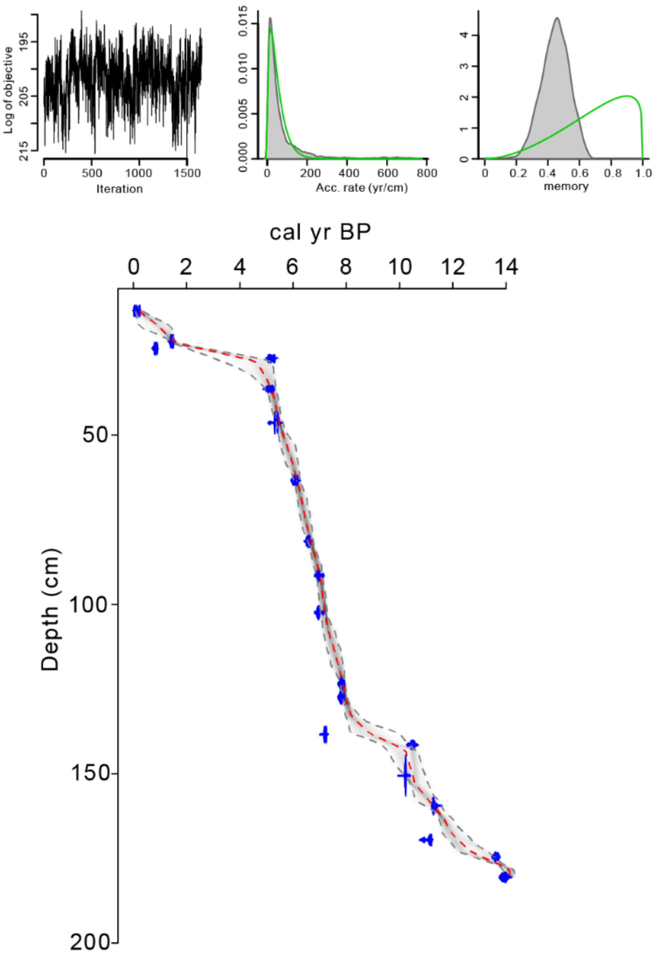

Fig. S10 Chorology of the ZGT peat core. Redraw after ref. 12.

References

1. Yue, Y. et al. A continuous record of vegetation and climate change over the past 50,000 years in the Fujian Province of eastern subtropical China. *Palaeogeogr. Palaeoclimatol. Palaeoecol.* **365–366**, 115–123 (2012).
2. Zhong, W., Cao, J., Xue, J., & Ouyang, J. A 15,400-year record of climate variation from a subalpine lacustrine sedimentary sequence in the western Nanling Mountains in South China. *Quat. Res.* **84**, 246–254 (2015).
3. Zhu, C. et al. Pollen record from Dajiuhu Basin of Shennongjia and environmental changes since 15.753 ka B.P. *Quat. Sci*. **26**, 814–826 (2006) (in Chinese with English abstract).
4. Zhou, W. et al. Postglacial changes in the Asian summer monsoon system: a pollen record from the eastern margin of the Tibetan Plateau. *Boreas* **39**, 528–539 (2010).
5. Zhao, Y., Yu, Z., Chen, F., & Zhang, J. Holocene vegetation and climate histories in the eastern Tibetan Plateau: controls by insolation-driven temperature or monsoon-derived precipitation changes? *Quat. Sci. Rev.* **27**, 1512–1525 (2008).
6. Volders, F. D. M. Biomarker Hydrocarbon Molecular and Deuterium Isotope Stratigraphic Records from Ombrotrophic Mires for Palaeoclimate Reconstruction. University of Bristol. PhD Dissertation (2003).
7. Li, C., Sessions, A. L., Kinnaman, F. S., & Valentine, D. L. Hydrogen-isotopic variability in lipids from Santa Barbara Basin sediments. *Geochim. Cosmochim. Acta* **73**, 4803–4823 (2009).
8. Fewster, R. E. et al. Holocene vegetation dynamics of circum-Arctic permafrost peatlands. *Quat. Sci. Rev.* **307**, 108055 (2023).
9. Yu, Z. Northern peatland carbon stocks and dynamics: a review. *Biogeosciences* **9**, 4071–4085 (2012).
10. Loisel, J. et al. A database and synthesis of northern peatland soil properties and Holocene carbon and nitrogen accumulation. *Holocene* **24**, 1028–1042 (2014).
11. Loisel, J. et al. Insights and issues with estimating northern peatland carbon stocks and fluxes since the Last Glacial Maximum. *Earth Sci. Rev.* **165**, 59–80 (2017).
12. Huang, X. et al. Holocene forcing of East Asian hydroclimate recorded in a

subtropical peatland from southeastern China. *Clim. Dyn.* **60**, 981–993 (2023).